chemistry proceedings

Proceedings

DNA-Binding Properties of Cytotoxic Naphtindolizinedione-Carboxamides Acting as Type II Topoisomerase Inhibitors. A Combined In Silico and Experimental Study †

Andrea Defant [1], Paolo Gatti [1], Alessandro Poli [1], Marta Serena [2], Alice Sosic [2], Barbara Gatto [2] and Ines Mancini [1,*]

[1] Laboratory of Bioorganic Chemistry, Department of Physics, University of Trento, Via Sommarive 14, 38123 Povo-Trento, Italy; andrea.defant@unitn.it (A.D.); paolo.gatti.1@alumni.unitn.it (P.G.); alessandro.poli@scuole.provincia.tn.it (A.P.)
[2] Department of Pharmaceutical and Pharmacological Sciences, University of Padova, via F. Marzolo 5, 35131 Padova, Italy; marta.serena87@gmail.com (M.S.); alice.sosic@unipd.it (A.S.); barbara.gatto@unipd.it (B.G.)
* Correspondence: ines.mancini@unitn.it
† Presented at the 24th International Electronic Conference on Synthetic Organic Chemistry, 15 November–15 December 2020; Available online: https://ecsoc-24.sciforum.net/.

Abstract: Some clinically-used anticancer drugs are DNA intercalators acting as topoisomerase (Topo) IIα poisons in tumor cells highly expressing the enzyme. Synthetic naphtindolizinedione-carboxamides, previously designed as potential antitumor agents and showing relevant cytotoxic activities in vitro, have been now evaluated for their DNA-binding and inhibition of human Topo IIα, in comparison with the drug mitoxantrone. Docking calculation of each synthetic molecule as ligand with the CGCGAATTCGCG oligonucleotide model showed a stable intercalation in the DNA cut inside the enzyme. Moreover, molecular dynamics simulation indicated the stability of each DNA complex by evaluating the H-bonds involved as a function of time. These results are correlated to spectroscopic (binding constants and melting temperature by UV–VIS analysis, circular dichroism) and biological data (cytotoxicity and inhibition of human Topo IIα decatenation assay).

Keywords: anticancer agent; docking calculation; molecular dynamics; spectroscopic methods

Citation: Defant, A.; Gatti, P.; Poli, A.; Serena, M.; Sosic, A.; Gatto, B.; Mancini, I. DNA-Binding Properties of Cytotoxic Naphtindolizinedione-Carboxamides Acting as Type II Topoisomerase Inhibitors. A Combined In Silico and Experimental Study. *Chem. Proc.* **2021**, *3*, 96. https://doi.org/10.3390/ecsoc-24-08103

Published: 13 November 2020

1. Introduction

For some planar intercalating ligands, including acridines, ellipticines, and doxorubicines, interaction with DNA is recognized to be essential for cytotoxicity, although it is not a sufficient condition. The in vitro tumor growth inhibition can actually be related to enzyme inhibition, as observed for several DNA intercalative agents showing reversible protein-linked DNA breaks when Topo II is involved. Topo II inhibition is able to promote cell death pathways and so stopping the tumor growth [1], a behavior which makes topoisomerase a useful target for the development of new potential drugs [2,3]. In mammalian cells two isoforms of the enzyme, α and β, are known. Some clinically-used antitumor drugs (doxorubicin, etoposide, and mitoxantrone) are DNA intercalating molecules acting as Topo IIα poisons in tumor cells highly expressing the enzyme [4]. The promising cytotoxic results obtained for compounds **1** and **2** have been the starting point for further studies.

Designed on the structural similarity with known antitumor agents as DNA intercalators (ellipticine, daunorubicin, mitoxantrone and 9-aminoacridine-4-carboxamide derivatives) [5,6], we reported on the novel naphtindolizinedione-carboxamides **1–3** (Figure

1), efficiently synthesized by a microwave-assisted multicomponent reaction [7]. Compounds **1** and **2** showed a good activity towards leukemia, and colon and renal cancer cells by the US National Cancer Institute (NCI) screening using a 60 human tumor cell line panel. The *N,N-syn* isomer **2** exhibited a very good selective inhibition against the melanoma MALME-3M cell line, with a GI_{50}-value (=65 nM) corresponding to a 283-fold increase in activity compared with the corresponding deaza-analogue **1** [6].

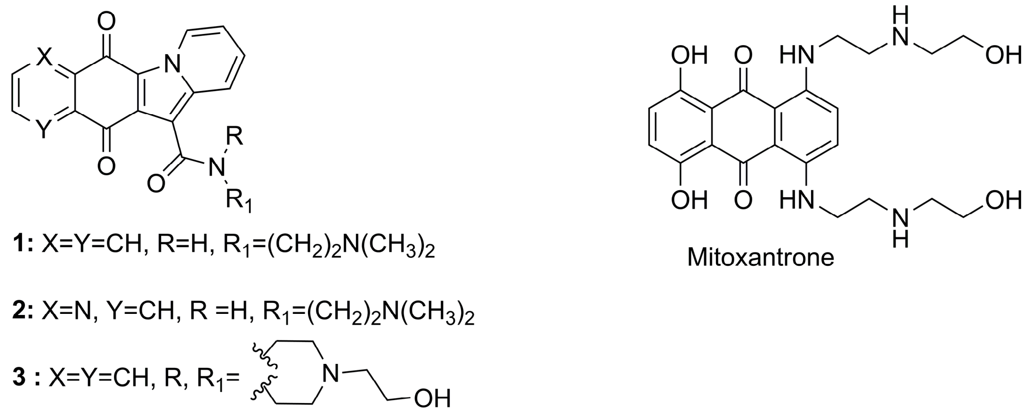

Figure 1. Molecular structures of molecules **1–3** under investigation and of the anticancer drug mitoxantrone.

We report here on the computational investigation of DNA interactions with **1–3** in their comparison with mitoxantrone (Figure 1), correlated to spectroscopic analysis and their evaluation in enzyme inhibition assay.

2. Materials and Methods

2.1. Molecular Docking

2.1.1. Calculations for the Protonated Ligand/Oligomeric DNA Complexes

They were performed on an Intel Pentium quad-core PC 2.8 GHz with 4 GB RAM by using Vina Docking (http://vina.scripps.edu/index.html) [8] associated with AutoDock Tools 1.5.6 (ADT) (http://mgltools.scripps.edu/downloads) [9,10], and the utilities AutoDock Helper, Vina Helper, and Energy Analyzer, belonging to the software suite D2MD, specifically created by one of the coauthors (P.G) for the study of DNA-ligand interactions and freely available [11]. For the calculation on the oligonucleotide, its crystallographic structure of the double strand oligonucleotide having sequence CGCGAATTCGCG is freely available from the Protein Data Bank (ID: 1BNA). All water molecules were removed and a molecules of ellipticine, taken as a template, was inserted between two pairs of GC bases in order to create the required space, by firstly performing an energy minimization using the Amber94 force field (parameterized for nucleotides) in Gromacs with the following parameters: define = -DFLEXIBLE, integrator = cg, nsteps = 2000, constraints = none, emtol = 1000.0, nstcgsteep = 10, emstep = 0.01, nstcomm = 1, coulombtype = PME, ns_type = grid, rlist = 1.0, rcoulomb = 1.0, rvdw = 1.4, Tcoupl = no, Pcoupl = no, gen_vel = no, nstxout = 0, optimize_fft = yes. Then, a further molecular dynamics calculation on the energy minimization output was performed by Gromacs (https://www.gromacs.org/) with the following parameters: integrator = md, nstep = 10000, -dt = 0.002, constraints = all-bonds, nstcomm = 1, ns_type = grid, rlist = 1.2, rcoulomb = 1.1, rvdw = 1.0, vdwtype = shift, rvdw-switch = 0.9, coulombtype = PME-Switch, Tcoupl = v-rescale, tau_t = 0.1 0.1, tc-grps = water non-water, ref_t = 300 300, Pcoupl = parrinello-rahman, Pcoupltype = isotropic, tau_*p* = 0.5, compressibility = $4.5 \cdot 10^{-5}$, ref_*p* = 1.0, gen_vel = yes, nstxout = 2, lincs-iter = 2, DispCorr = EnerPres, optimize_fft = yes**.** Ellipticine was manually removed and the new structure of double-strand DNA with the appropriate space between CG bases was saved as a PDB file. Docking calculations was performed putting each molecule in the preformed space for compounds **1–3**, whereas in blind mode for mitoxantrone. The grid box dimensions for Vina calculations were set to 13.389 Å × 13.389 Å × 13.389 Å for compound **1**, 13.944 Å × 13.944 Å × 13.944 Å for **2**, 16.008 Å × 16.008 Å × 16.008 Å for **3** and 25.368 Å × 26.239 Å × 47.537 Å for mitoxantrone. Docking simulations were achieved by Vina Docking and AutoDock Helper and the resulting ligand docked conformation free energies and binding constants were treated by Energy Analyzer. All the AutoDock Helper computations were performed using the AutoDock default parameters and setting the number of runs to 100. All Vina Docking simulations were performed using the parameters: exhaustiveness = 128, number of conformations to keep = 20, and allow torsions of amide groups = yes.

2.1.2. Docking Calculation on Topoisomerase II

The crystal structure of the enzyme was available as a PDB file (ID 3QX3), composed by the core part of the enzyme plus a twenty base pair DNA with two intercalated molecules of Etoposide, and six Mg^{2+} ions. The docking simulations were performed by AutoDock Helper and Vina Helper, with the same procedure and parameters used in the previous docking calculations on the oligonucleotide. For obtaining reliable results, the docking process was validated before use. For this purpose, etoposide was removed from the enzyme and docked again in the same original structure. The resulted etoposide conformation well superimposed with the original one by performing AutoDock simulations, whereas Vina resulting conformation was not.

2.2. Molecular Dynamics

It was performed using Gromacs and choosing the force field Amber94 for both DNA and the ligand. The chosen water model was tip3p, the water box symmetry was set as triclinic and the distance between the complex and the box = 1 nm. Total charge of the DNA/ligand complex immersed in water was −21 for compounds **1–3** and −20 for mitoxantrone. In order to reset the complex charge to 0, a variable number of Na^+ and Cl^- ions was added to the system with a concentration of 0.15 mol·L^{-1}. The parameters adopted in the calculations were: number of steps = 10^7, time step = $2 \cdot 10^{-15}$ s, neighbors search type = grid, neighbors list cut-off distance = 1.27 nm, electrostatics model = PME-Switch, coulomb distance cut-off = 1.1 nm, van der Waals interactions model = shift, van der Waals distance cut-off = 1.0 nm, van der Waals switching threshold = 0.9 nm, temperature coupling = v-rescale, time constant for temperature coupling = 0.1 ps, reference temperature = 300 K, pressure coupling = Parrinello-Rahman, pressure coupling type = isotropic, period of pressure fluctuations = 0.5 ps, reference pressure = 1 bar, compressibility = $4.5 \cdot 10^{-5}$ bar^{-1}, dispersion corrections = energy + pressure.

3. Results and Discussion

3.1. Computational Study

It was performed on a crystallographic DNA structure (from PDB file). Docking calculations for DNA complexes with each **1**, **2** or **3** provided the values for the corresponding binding constants (Table 1). A visual inspection of the complexes indicated that the ligand 1 was stabilized by stacking interactions with DNA nucleotides and by formation of two H-bonds involving its amide group and two oxygen atoms of the DNA backbone (Figure 2). The DNA/2 complex showed only one H-bond between the amide unit and the sugar-phosphate moiety and a further H-bond between the protonated dimethylamine group and the oxygen of a DNA cytosine unit. For compound **3**, the complex displayed a single interaction involving the OH group present in the piperazine chain and an oxygen atom in the DNA sugar moiety, attesting a minor interaction (Figure 2). Mitoxantrone gave an intercalation stabilized by four H-bonds between one chain and the oxygen atoms of the DNA backbone, added to a minor groove interaction by one H-bond between an aminium group and the DNA backbone (Figure 3). A comparison with the experimental data (reported below) showed a good agreement for

Table 1. Values obtained by docking calculations for complexes of the indicated compounds in protonated form with $(CGCGAATTCGCG)_2$ oligomer.

Ligand	ΔG (Kcal/mol)	K
1	−8.4	$1.4 \cdot 10^6$
2	−8.5	$1.7 \cdot 10^6$
3	−9.1	$5.0 \cdot 10^6$
Mitoxantrone	−7.8	$1.5 \cdot 10^5$

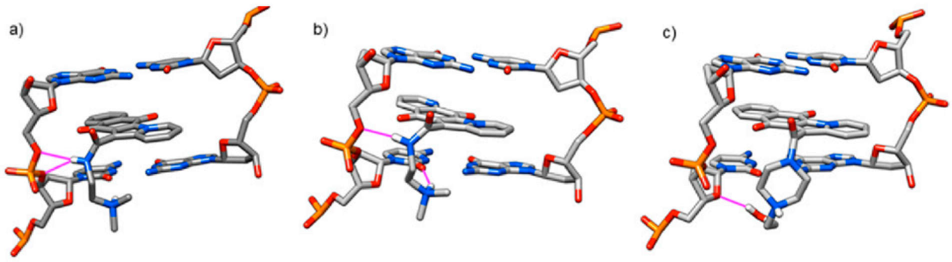

Figure 2. View of DNA (PDB ID: 1BNA) docked conformations of compounds: (**a**) **1**, (**b**) **2** and (**c**) **3** in protonated forms. H-bridges are drawn in magenta.

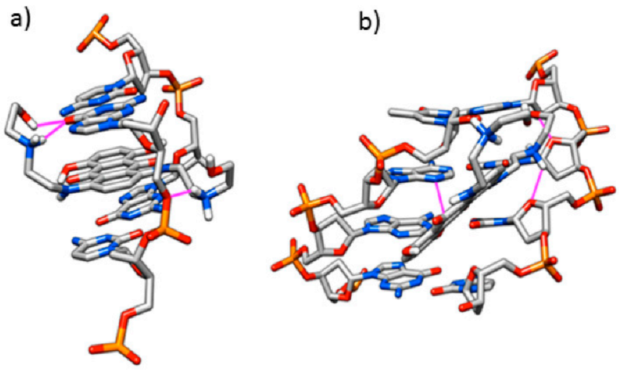

Figure 3. View of DNA (PDB ID: 1BNA) docked conformations of mitoxantrone in protonated form: (**a**) intercalated and (**b**) inserted in the minor groove. H-bridges are drawn in magenta.

1, **2** and mitoxantrone, whereas an overestimated value was observed for **3**, which requires the further approach by molecular dynamics simulation.

The availability of the X-ray crystal ternary structure of the human enzyme in complex with an oligonucleotide and etoposide gave us the opportunity to calculate the interaction with molecules **1** and **3**, taken into account without protonation of the tertiary amine, in line with the form involved in the enzymatic assay reported below, carried out under basic conditions. Based on a visual inspection, **1** was intercalated in the cut DNA, showing the amide group involved in a H-bond with oxygen of the DNA skeleton. The break was mediated by TYR 821, which cuts the nucleic strand forming a covalent bond with a DNA backbone phosphate group. The supposed relegation process cannot occur, because **1** was stably intercalated. A further calculation was carried out on protonated amine, obtaining similar results. The most notably difference was the presence of a further H-bond between the trialkylaminium group and DNA backbone oxygen (Figure 4).

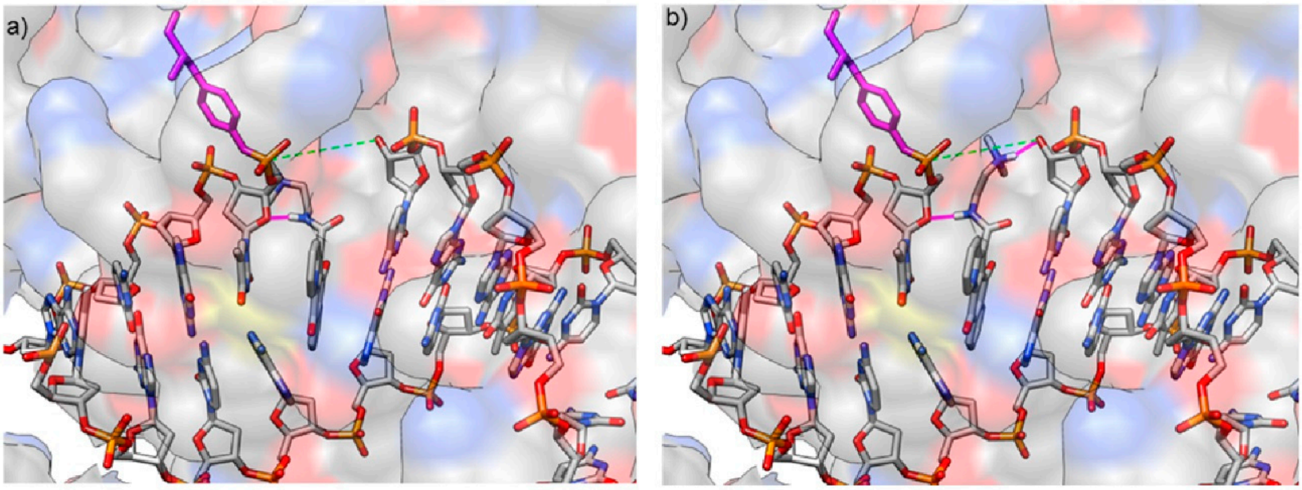

Figure 4. 3D View of DNA-intercalated compound **1**: (**a**) in free form, and (**b**) in protonated form.

In summary, docking simulations indicated that ligand **1** acted as a Topo II poison, stabilizing the cleavage complex and inducing permanent breaks in the system.

Molecular dynamics (MD) allowed a more realistic view on the supramolecular system, taking into account molecular motions during the simulation time. The small Root Mean Square Deviation (RMSD) values obtained for DNA/ligand complexes reported in Table 2 are indicative for a stable system, where the complexes remained stable for all the simulation time (Figure 5).

Table 2. Values by MD simulations for the indicated ligands as protonated form in the complexes with $(CGCGAATTCGCG)_2$ oligomer.

Ligand	Ligand RMSD [nm]	Oligomer RMSD [nm]	H-bond Number
1	0.14	0.29	0.532
2	0.11	0.26	0.342
3	0.13	0.21	0.060
Mitoxantrone (intercalation)	0.09	0.25	2.672
Mitoxantrone (minor groove interaction)	0.11	0.22	3.756

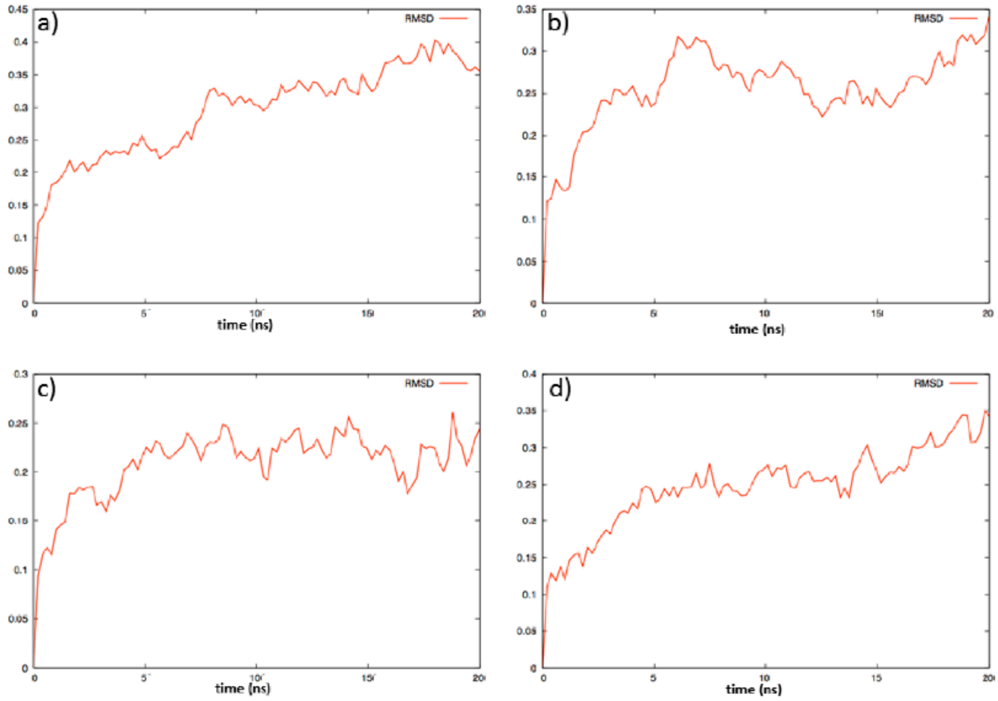

Figure 5. Root-mean-square deviation (RMSD) graphs obtained by molecular dynamics simulation showing the variation as a function of time of DNA (PDB ID: 1BNA) shapes interacting with each ligand: (**a**) **1**, (**b**) **2**, (**c**) **3**, and (**d**) mitoxantrone.

An indication of the interaction stability in DNA complexes could be deduced by the evaluation of H-bond number involved for each ligand in function of the time (Table 2, Figure 6). In the case of **1** and **2** a sustained presence of at least one H-bond stabilizing the corresponding DNA complex was observed. The known interaction of mitoxantrone by its two amine groups present in the side chains, able to produce a more stable complex, was also validated by the presence of a higher number of H-bonds. They were involved in intercalation and minor groove interaction and were stable during the simulation time. When DNA/**3** complex was analyzed, the found H-bond was almost absent for all the MD simulation time. Therefore, MD simulations showed that **3** intercalated more weakly than the other ligands, since as soon as the DNA/**3** complex interacted with Topo II, the ligand was not stable enough to remain intercalated and was expelled from the nucleic acid and from the cleavage. This result gave an explanation of the overestimated binding deduced by docking calculation (Table 1, Figure S1) which allowed to observe only one snapshot of the system, not representative for the real behavior of the DNA/ligand complex.

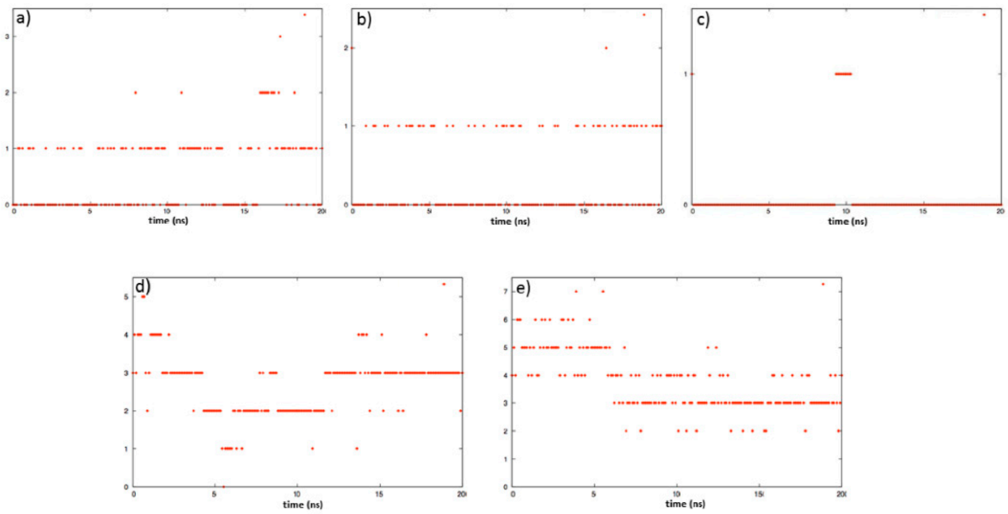

Figure 6. H-bond number in function of the time involved for each ligand with DNA: (**a**) **1**, (**b**) **2**, (**c**) **3**, (**d**) intercalated mitoxantrone, and (**e**) mitoxantrone interacting in the minor groove.

3.2. Spectroscopic Analyses

Calf thymus DNA complexes with each compound **1–3** as hydrochloride salts (obtained by treatment with one molar equivalent of conc HCl in absolute ethanol at 0 °C for 30 min, followed by in vacuo evaporation) were investigated by UV–VIS spectroscopy (Supplementary and Figure S2). The corresponding equilibrium constants of interaction [12,13 were compared with the data for DNA/mitoxantrone complex (Table S1). Each ligand interacted with DNA, with **1** and **2** giving ten-fold higher values than both mitoxantrone and **3**.

DNA thermal denaturation based on melting temperature (T_m) analysis gave values for **1** and **2** which were comparable to mitoxantrone and higher than compound **3** (Figure S3 and Table S1). These indications on the stabilizing effect by ligand **1** or **2** on the double strand DNA support the fact that in the presence of a strong interaction, T_m increases proportionally to the binding strength [14]. Based on this comparative analysis, **1** and **2** emerged as the best interacting molecules, clearly distinct from **3** which structurally differs in the side chain.

As a very simplified model for calf thymus DNA (containing a 55% CG bases), the same dodecameric synthetic oligonucleotide $(CGCGAATTCGCG)_2$ (with a 67% CG bases, Supplementary) taken into account in the computational study, was also used with compound **2**. The corresponding complex was investigated by UV spectra and a qualitative behavior in agreement with the complex involving the natural DNA was obtained.

A complementary approach to the study of DNA interactions is given by circular dichroism (CD), which allows the detection of changes in DNA absorption bands induced by achiral ligands. In addition, it is able to establish the kind of interaction, where the strongest is intercalation deriving by insertion of the ligand, which causes a distortion of the double helix changing the relative positions of the bases [15]. CD analysis (Supplementary) was carried out at a constant DNA concentration by the additional presence of increasing amounts of each ligand **1–3** and mitoxantrone. When DNA complexes were regarded using comparable concentrations of each ligand, CD spectra showed an increasing of molar ellipticity caused by a base stacking of the helix distortion for the band at 275 nm (which is linearly related to the helix winding angle [16]), as well as an increasing due to the hydrogen bond alterations among the bases of the negative band around 242 nm (Figure S4). If compared with the spectrum for free DNA, compounds **1–3** caused a very small hypsochromic shift on the negative Cotton band and a more consistent shift (10 nm) on the positive one. The data supported a DNA intercalation mode [17, where the ligand plane is orthogonal to the phosphate sugar backbone and the aromatic structure of the tested compounds finds position between two adjacent bases. Electronic transitions polarized in the aromatic plane of compounds **1–3** will, therefore, preferentially absorb light that is linearly polarized with an orthogonal plane to the nucleic acid backbone axis [18. Mitoxantrone is responsible for more considerable changes in the three-dimensional structure of DNA, as deduced by more pronounced alterations in molar ellipticity values, as well as by a 3 nm hypsochromic shift in negative band and a comparable bathochromic shift in the positive one. These data are in line with a dual mode of interaction, including intercalation, and groove interaction [18].

The trend shown by these spectroscopic data is in line with both the finding from the computational study and the lowest cytotoxicity of **3**. The combined evidence supports the decisive role played by the *N,N*-dimethylethylamino chain present in **1** and **2**, which represents really the most significant structural modification to promote the cytotoxicity [5,6].

3.3. Topoisomerase IIα Activity

The decatenation assay is based on the ability of human topoisomerase II to convert a concatenated DNA in its decatenated form. This enzyme is able to alter DNA topology by catalyzing the passing of an intact DNA double helix through a transient double-stranded break made in a second helix and it is critical for the resolution of torsional problem during several cellular events. The inhibition by compounds **1–3** of Topo IIα, which is highly expressed in cells undergoing division, could be correlated to the promising cytotoxic results obtained from previous studies, as to the computational and spectroscopic analyses herein reported. In inhibition of human Topo IIα decatenation assay [19, (Supplementary) only **1** and **2** were able to give positive results (Figure S5), as observed in comparison with mitoxantrone (Figure S6), supported by IC_{50} values evaluated for each compound and mitoxantrone taken as a control, which showed an inhibition at low concentrations of **1** and **2**, but no activity for compound **3** up to 100 μM (Table S2).

Once again, the obtained data suggest that the presence of a *N,N*-dimethylethylamino side chain (present in **1** and **2**) is a fundamental requirement for activity of these compounds. Furthermore, the planar structure of the ring system, typical of intercalating agents, suggests that probably they act as Topo II poisons, stabilizing the cleavage-complex. Binding data, in fact, show that **1** and **2** strongly interact with DNA through intercalation, although the presence of nitrogen into the planar nucleus of compound **2** seems to slightly decrease the activity. Moreover, the interactions for the human enzyme in complex with an oligonucleotide and not protonated **1** and **3** previously calculated can be correlated to the condition involved in the enzymatic assay carried out at pH = 7.9. The evidence of a stable intercalation in the DNA cut inside the enzyme is in line with the inhibition of human Topo IIα resulted for **1** (IC_{50} = 1.78 μM) higher than mitoxantrone (Table S2). However, its highest inhibition of human topoisomerase does not match fully with the most potent and selective cytotoxicity observed for **2** against melanoma cell line, indicating that a further mode of action or selective uptake must be involved in the case of this aza analogue.

4. Conclusions

Synthetic naphtindolizinedione-carboxamides **1** and **2**, previously designed as potential antitumor agents by showing in vitro promising cytotoxic activities, have been investigated in their interaction with DNA and acting as Topo II inhibitors. The computational approach based on a synthetic oligonucleotide model, included molecular docking calculation showing the intercalation of **1** in the DNA cut inside the enzyme, able to support its mechanism as an inhibitor of this enzyme. MD simulation provided indications of DNA complexes stability by evaluating the H-bonds involved for each ligand in function of the time. The results fit both the lowest cytotoxicity observed for **3** and the spectroscopic data. DNA-binding properties of **1–3** in comparison with mitoxantrone have been evaluated by UV–VIS spectroscopy, including equilibrium constants and thermal denaturation of their corresponding DNA complexes. The mode of interaction has been also deduced from CD spectra following the ellipticity changes caused by compounds **1–3** on calf thymus DNA, as well as on the same oligonucleotide. considered in the computational approach. In addition, the in silico evidence is correlated to the inhibition of human Topo IIα decatenation, where **1** and **2** exhibited activities comparable to mitoxantrone. Otherwise, compound **3** was inactive, in line with both the evaluation of binding constant and inactivity in cytotoxicity assays, and MD simulation showing that more weakly intercalation than the other ligands.

Supplementary Materials: The following are available online, **Figure S1:** View by docking calculation of compound **3** interacting inside the topoisomerase II (PDB ID: 3QX3) cleavage site: in free base form (**a**) and in protonated form (**b**). The tyrosine residue mediating DNA cut is drawn in magenta, H-bridge is shown by green circles, the phosphate-deoxyribose bond broken by tyrosine is depicted in green dashed line, **Figure S2:** UV–VIS spectra used for the calculation of molar extinction coefficient, recorded in 240–500 nm range, for buffer solutions (Tris-HCl 10 mM, NaCl 20 mM, pH = 7.5) of compounds: (**a**) 1, (**b**) 2, (**c**) 3, **Figure S3:** DNA thermal denaturation based on melting temperature (Tm) analysis by compound 1–3 in comparison with mitoxantrone, **Figure S4:** Overlapped CD spectra of DNA complexes using comparable concentrations of each ligand 1–3 and mitoxantrone, in comparison with the spectrum of free calf thymus DNA, **Figure S5:** Inhibition of human topoisomerase IIα decatenation assay by compounds **1–3** used at increased concentrations (0.1–1-10–100 μM); B, blank; C, control (+enzyme), **Figure S6:** Inhibition of human topoisomerase IIα decatenation assay by mitoxantrone, **Table S1:** Equilibrium constants and Tm values for the indicated calf thymus DNA complexes, in 10 mM TRIS buffer solution, using each ligand as hydrochloride salts, **Table S2:** Inhibition of human topoisomerase IIα decatenation assay IC50 values for 1–3 and mitoxantrone.

Author Contributions: Conceptualization: A.D. and I.M.; methodology: A.D., I.M., and B.G.; software: A.D. and P.G.; validation: P.G., A.D., M.S., A.S., and A.P.; formal analysis: A.P., P.G., M.S., and A.S.; investigation: A.D., P.G., and A.P.; data curation: A.D., P.G., A.P., and B.G.; writing—original draft preparation: I.M., A.D., and B.G.; writing—review and editing: I.M. and A.D.; supervision: I.M. All authors have read and agreed to the published version of the manuscript.

Funding: This research received no external funding.

Institutional Review Board Statement: Not applicable

Informed Consent Statement: Not applicable.

Data Availability Statement: Not applicable.

Acknowledgments: We thank Mario Rossi, University of Trento for his technical support and we are grateful to Lorenzo Lunelli, Bruno Kessler Foundation (FBK), Trento for the use of UV spectrophotometer equipped with a thermostatic unit.

Conflicts of Interest: The authors declare no conflict of interest.

Sample Availability: Samples of the compounds are available from the authors.

References

1. Deweese, J.E.; Osheroff, N. The DNA cleavage reaction of topoisomerase II: Wolf in sheep's clothing. *Nucleic Acids Res.* **2009**, *37*, 738–748, doi:10.1093/nar/gkn937.
2. Martinez, R.; Chacon-Garcia, L. The Search of DNA-Intercalators as Antitumoral Drugs: What it Worked and What did not Work. *Curr. Med. Chem*. **2005**, *12*, 127–151, doi:10.2174/0929867053363414.
3. Wu, C.C.; Li, T.K.; Farh, L.; Lin, L.Y.; Lin, T.S.; Yu, Y.J.; Yen, T.J.; Chiang, C.W.; Chan, N.L. Structural basis of type II topoisomerase inhibition by the anticancer drug etoposide. *Science* **2011**, *333*, 459–462, doi:10.1126/science.1204117.
4. Heck, M.M.; Earnshaw, W.C. Mitotic chromatin condensation in vitro using somatic cell extracts and nuclei with variable levels of endogenous topoisomerase II. *J. Cell Biol.* **1986**, *103*, 2569–2581, doi:10.1083/jcb.111.6.2839.
5. Defant, A.; Guella, G.; Mancini, I. Synthesis and in vitro cytotoxicity evaluation of novel naphthindolizinedione derivatives. *Arch. Pharm. Chem. Life Sci.* **2007**, *340*, 147–153, doi:10.1002/ardp.200600160.
6. Defant, A.; Guella, G.; Mancini, I. Synthesis and *in-vitro* cytotoxicity evaluation of novel naphtindolizinedionederivatives, part II: Improved activity for aza-analogues. *Arch. Pharm. Chem. Life Sci.* **2009**, *342*, 80–86, doi:10.1002/ardp.200800177.

7. Defant, A.; Guella, G.; Mancini, I. Microwave-assisted multicomponent synthesis of aza-, diaza-, benzo-, and dibenzofluorenedione derivatives. *Synth. Commun.* **2008**, *38*, 3003–3016, doi:10.1080/00397910802044249.
8. Trott, O.; Olson, A.J. AutoDock Vina: improving the speed and accuracy of docking with a new scoring function, efficient optimization and multithreading, *J. Comput. Chem.* **2010**, *31*,455-461, doi:10.1002/jcc.21334.
9. Sanner, M.F. Python: A Programming Language for Software Integration and Development. *J. Mol. Graph Model.* **1999**, *17*, 57-61.
10. Morris, G. M.; Huey, R.; Lindstrom, W.; Sanner, M. F.; Belew, R. K.; Goodsell, D. S.; Olson, A. J. Autodock4 and AutoDockTools4: automated docking with selective receptor flexibility. *J. Comput. Chem.* **2009**, *16*, 2785-2791, doi: 10.1002/jcc.21256.
11. Available online: https://code.google.com/archive/p/d2md/downloads (accessed on 20 October 2020).
12. Strat, D.; Missailidis, S.; Drake, A.F. A novel methodological approach for the analysis of host-ligand interactions. *ChemPhysChem* **2007**, *8*, 270–278, doi:10.1002/cphc.200600442.
13. Stootman, F.H.; Fisher, D.M.; Rodgerc, A.; Aldrich-Wright, J.R. Improved curve fitting procedures to determine equilibrium binding constants. *Analyst* **2006**, *131*, 1145–1151, doi:10.1039/B604686J.
14. Mergny, J.-L.; Lacroix, L. Analysis of thermal melting curves. *Oligonucleotides* **2003**, *13*, 515–537, doi:10.1089/154545703322860825.
15. Lerman, L.S. Structural considerations in the interaction of DNA and acridines. *J. Mol. Biol.* **1961**, *3*, 18–30, doi:10.1016/S0022-2836(61)80004-1.
16. Johnson, B.B.; Dahl, K.S.; Tinoco, I.; Ivanov, V.; Zhurkin, V.B. Correlations between deoxyribonucleic acid structural parameters and calculated circular dichroism spectra. *Biochemistry* **1981**, *20*, 73–78.
17. Rajendran, B.U.A. Nair. *Biochim. Biophys. Acta* **2006**, *1760*, 1794–1801, doi:10.1021/bi00504a013.
18. Garbett, N.C.; Ragazzon, P.A.; Chaires, J.B. Circular dichroism to determine binding mode and affinity of ligand–DNA interactions. *Nat. Protoc.* **2007**, *2*, 3166–3172, doi:10.1038/nprot.2007.475.
19. Furlanetto, V.; Zagotto, G.; Pasquale, R.; Moro, S.; Gatto, B. Ellagic acid and polyhydroxylated urolithins are potent catalytic inhibitors of human topoisomerase II: An in vitro study. *J. Agric. Food Chem.* **2012**, *60*, 9162–9170, doi:10.1021/jf302600q.